Autonomous Flow-Through RGB and Hyperspectral Imaging for Unmanned Surface Vehicles

1st Matias Haugum
Department of Engineering Cybernetics
Norwegian University of Science and Technology
Trondheim, Norway
matias.haugum@ntnu.no

2nd Glaucia Moreira Fragoso
Department of Biology
Norwegian University of Science and Technology
Trondheim, Norway
glaucia.m.fragoso@ntnu.no

3rd Marie Bøe Henriksen
Department of Engineering Cybernetics
Norwegian University of Science and Technology
Trondheim, Norway
marie.b.henriksen@ntnu.no

4th Artur Piotr Zolich
Department of Engineering Cybernetics
Norwegian University of Science and Technology
Trondheim, Norway
artur.zolich@ntnu.no

5th Tor Arne Johansen
Department of Engineering Cybernetics
Norwegian University of Science and Technology
Trondheim, Norway
tor.arne.johansen@ntnu.no

***Abstract*—The process of collecting samples for traditional microscopic analyses can be costly and time-consuming. We present the design of an autonomous flow-through imaging (AFTI) system tailored for small unmanned surface vehicles (USVs). Called the 'AFTI-scope', the design is built around readily available microscopy parts. A peristaltic pump is used to move a water sample through a channel slide, which is positioned beneath a magnifying objective. Stepper motors give accurate control of the stage position and focus. An RGB-microscope camera images continuously the suspended microorganisms and other particles as they flow through the channel. Moreover, by using a stepper motor to pan the stage, hyperspectral datacubes were captured using a push-broom hyperspectral camera fixed to one of the eyepiece tubes of the microscope, which provides spectra of the particles that can be useful for classification. To segment the images for later classification and identification, an image processing pipeline is employed to perform various manipulations on the images, such as removing any particles that may have become stuck, subtracting the background, and normalizing the images. The resulting data set is a prime candidate for segmentation and quantification of particles. After segmentation, the reduced data set can either be sent to a taxonomist for identification or fed into algorithms for classification. Tests from plankton net samples showed that the system is capable of imaging suspended particles with a resolution of 0.41 µm/pixel at flow rates up to 7.8 ml/min. For the given setup, an image size 1280x960 pixels provides the best trade-off between resolution and frame rate, producing the clearest pictures with the least amount of motion blur.**

***Index Terms*—In-situ sampling, Autonomous Vehicles, Oceanography, HABs, Hyperspectral Sensors**

I. Introduction

A. Algal Blooms

Algal blooms are phenomenona where the amount of phytoplankton rapidly increase due to ideal growth conditions. Certain species of phytoplankton may, in large numbers, be harmful to marine life. This can be due to innate characteristics, or through the production of toxins. As an example, certain species of the diatom genus *Chaetoceros* have long *setae*; spiny 'hair-like' features that can cause irritation to the gills of fish [1]. Cyanobacteria, also known as *blue-green algae*, can under certain conditions produce toxins. These toxins may cause harm to humans, pets and livestock through direct exposure, or indirectly through filter-feeders such as mussels and clams where they may accumulate. Such blooms are called harmful algal blooms (HABs) and can inflict significant damage to marine life as well as the economy of the aquaculture industry. Although satellite imagery can detect the presence of algal blooms in surface waters from space, identifying the specific species responsible for the bloom requires the expertise of a skilled taxonomist.

Microscopic analyses (identification and quantification) of algal species require expertise and can be time-consuming. If the samples are to be retrieved from the open waters, transport (boat) and personnel will be required. In addition, if the samples are to be analyzed in a lab, additional time from collection to analysis must be expected. Once the underlying species is identified, the characteristics of the bloom can be evaluated to determine whether it poses a threat to marine life. However, urgency is of utmost importance if the bloom

be situated close to a fish farm. If the bloom is harmful, the stock of the fish farm may be at risk, and measures must be carried out to ensure that the stock is not lost. This may require either moving the net, stop feeding to reduce high fish density near the surface, or slaughter the stock prematurely. If the stock dies of because of exposure to algae toxins, it cannot be sold as food.

B. Autonomous Water Sampling

Utilizing unmanned surface vehicles (USVs) can result in significant savings in terms of time and cost, as compared to deploying dedicated vessels with personnel aimed to collect and analyze the water samples. The USV could be directed to a point of interest and collect a water sample. If the vehicle carries the correct equipment, an in-situ analysis can be carried out immediately. By imaging the particles in the water sample under magnification, the resulting images could either be analysed onboard using machine vision, or be transmitted for onshore analysis, where both options are saving a significant amount of time and work as opposed to collecting and analyzing the water samples manually. In this paper, the design of a flow-through imaging system built specifically for autonomous vehicles is presented. The design is based around readily accessible microscopy parts, using a microscope as a foundation. A peristaltic pump moves the water sample with great control through a channel slide situated beneath a magnifying objective. Furthermore, cameras can be fixed to the eyepiece tubes of the microscope to continuously image the suspended particles in the water sample as they flow through the channel. Other sensors can be attached to the system as well, catering to a wide range of use cases. As an example, a hyperspectral imager can be fixed to the system to capture hyperspectral data. When operating in remote regions, it may be necessary to adjust the focus to guarantee good images during operation. For this reason, stepper motors are installed to grant control over the focus distance, as well as the stage position. The focus-stepper not only allows a remote adjustment of the focus, but also advanced imaging methods such as phase imaging [2]. The ability to control the stage position also facilitates the capture of hyperspectral data, as the stage can be slowly moved while the sensor records in a push-broom manner.

After sampling, an image processing pipeline further refines the images by filtering out the images of material stuck to the slide, and normalizing the background. After capturing the images, thresholding techniques can be used to create binary masks from them, which are ideal inputs for algorithms for analysis and classification. By using unsupervised classification, it becomes possible to group different species, allowing for their quantification.

C. Related work

Similar systems already exist, ranging from accessible open-source citizen grade to high-end state of the art scientific instruments. An example of an open-source system is the *PlanktoScope* [3]. Built around a Raspberry Pi, the PlanktoScope enables citizen scientists to image small particles (>few μm) without having to look into a microscope. Intended for both researchers and non-researchers, the PlanktoScope is built around readily available parts in order to be a low-cost solution for anyone that wants to image phytoplankton. While it is an affordable ($\sim$ USD 500) all-in-one solution, but is also limited in terms of its hardware. The camera used in the PlanktoScope is the PiCamera, with a lens providing the magnification. This yields a resolution of 2.8 μm/pixel, sampling at a rate of 1.8 ml/min. Changing the magnification requires disassembly of the module and swapping of the lens. The performance of the Raspberry Pi also puts limits on the camera resolution, and highest achievable framerate. What the PlanktoScope lacks in hardware, it makes up for in functionality. Using the Python library MorphoCut, [4] the images are segmented and prepared for uploading to EcoTaxa, a web application for taxonomic annotation of images [5].

On the opposite side end of the spectrum is the SilCam, which is an instrument for in-situ imaging of suspended particles. Using holographic imagery instead of lens-based imaging, the SilCam overcomes depth-of-field and perspective related errors. Furthermore, the SilCam is capable of identifying suspended particles using a deep convolutional neural network. A study carried out by A. Saad, E. Davies and A. Stahl in 2020 performed an in-situ classification on images captured by the SilCam, dividing them between classes such as zooplankton, diatom chains, and fish eggs. In addition, a quantification of these particles can be carried out, yielding size distributions and concentrations of the particles [6]. However, a drawback of the SilCam is its inability to image smaller particles, and it is thus better suited for imaging larger particles such as large phytoplankton and zooplankton in sizes 50μm and up.

The application of machine learning techniques to differentiate among species is not a recent development. In 2007, researchers H.M Sosik and R.J Olson conducted a study in which images from an Imaging FlowCytoBot were utilized as input for a machine learning algorithm to classify specimens into 22 distinct categories. The resultant classification model achieved levels of accuracy ranging from 66% to 99% across the various classes [7]. The Imaging FlowCytoBot was also used in a study where dinoflaggelates of *Dinophysius Ovum* and *Mesodinium spp.* were monitored over several years in an attempt to predict the potential harmful algal blooms they could cause. The study found that the presence of *Mesodinium* in combination with environmental conditions could be used to predict future blooms of *D. Ovum* [8].

D. Contribution

Compared to the PlanktoScope, the AFTI-scope comes at a greater hardware cost at approximately 1800 Euro for the RGB-version, but is still significantly cheaper to other systems such as the Imaging FlowCytoBot priced at an approximate cost of USD 158 000 [9]. Depending on the cameras installed, the AFTI-scope is capable of imaging at resolutions catering

to a wide range of particle sizes. With a 1.23MP camera recording at 1280x960 pixels, a resolution of 0.82 µm/pixel is achieved compared to the PlanktoScopes resolution of 2.8 µm/pixel, recording at comparable framerates (approximately 30FPS). The increased resolution makes the AFTI-scope better suited for imaging smaller particles such as smaller phytoplankton, but may also be configured for larger particles such as zooplankton by changing the magnification. Furthermore, compared to the PlanktoScope, fewer parts are needed and thus less assembly is required. In addition, the light condenser may be changed to enable darkfield microscopy for increased contrast.

Multiple eyepiece-tubes allow for installing different cameras and sensors based on the needs of the mission. The recent progress in the development of low-cost hyperspectral imagers [10], [11] is an enabling technology that we want to exploit, since it can increase the available scientific information from the sensing system.

II. Proposed solution

Due to the small size of some particles (1 µm - 1mm), imaging under magnification is required. Furthermore, it is necessary to transport the water sample to the stage under the field of view of the cameras. This section presents the proposed design of the system. Citizen grade microscopy parts provide the optics and magnification, and a dosing pump is used together with a channel slide and silicone tubing to move the sample. Stepper motors manipulate the focus and stage position. A drawing of the AFTI-scope is shown in Fig. 1.

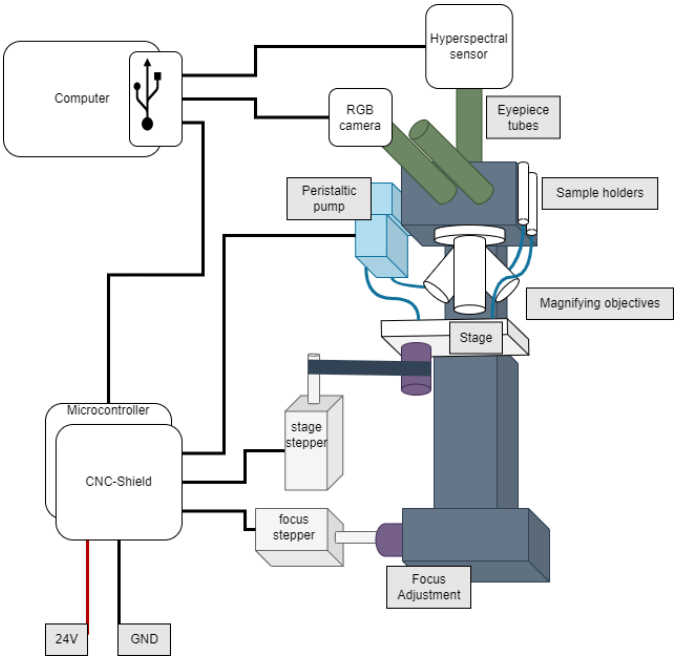

Fig. 1. Circuit drawing of the connections in the system. The microcontroller and cameras connect to the computer using USB-cables. The CNC-shield mates directly to the microcontroller, communicating through the headers. The phases of the stepper motors connect to the CNC-shield, and are mechanically attached to the microscope using belt- and direct drives. The peristaltic pump receives power and step signals from the CNC-shield.

A. Hardware

The base component for the proposed system is a desk microscope. Often made out of cast iron, the microscope offers a stable foundation for attaching a wide variety of components to it. Some microscopes has a changeable *light condenser*, and can use a stock abbe-condenser as well as a darkfield condenser for increased contrast. The eyepiece tubes on the microscope permit the mounting of several sensors simultaneously. A revolving turret with objectives of different magnifications permit capturing images at selected magnifications.

A peristaltic dosing pump transports the water sample from the sample reservoir to a transparent Ibidi channel slide located below the microscope objective, allowing for the contents of the sample to be imaged. These channel slides come at different depths of 0.2 mm, 0.4 mm, 0.6 mm and 0.8 mm, depending of the target particle size to be image. Shallower depths have the advantage of reducing the flow cell, and is ideal for imaging nanoplankton (<20 µm in size), keeping the specimen in the correct focus range, but the reduced volume in turns increases the fluid velocity, for a given volumetric flow rate. As gravity keeps most particles against the bottom of the channel slide, the larger volume slides are preferred. Silicone tubing connects all the fluid parts in the system. The inner tubing of the peristaltic pump may be changed catering for different flow speeds.

A micro-controller running the open-source CNC-firmware GRBL is used to control the stepper motors and the pump in the system. The micro-controller receives serial commands via an USB cable, translating it to the stepper signals sent to the motors. Attached to the micro-controller is a CNC-shield with stepper motor drivers. The CNC-shield is a printed circuit board that mates directly to the headers of the microcontroller, providing both power and an interface for the stepper motors. There are several advantages of using GRBL in combination with the CNC-shield; on the hardware level, *microstepping* can be enabled by shorting headers on the stepper drivers, such that higher stepping resolutions are achieved. This is useful for sensitive parts such as the stepper attached to the focus, allowing it to be moved with great precision. On the software level, parameters such as number of steps per millimeter, motor acceleration and so on can be fine tuned. The system operates on 24V, and the input power is supplied through the CNC-shield.

III. Implementation

A. Hardware

The microscope used in this design is the Bresser Science TFM-301 Trino microscope, shown in Fig. 2. The microscope has three eyepiece tubes on which sensors can be fitted. A revolving objective turret with 4 different magnifications is incorporated in the system. These objectives offer magnifications at 40x, 100x, 400x and 1000x respectively. The light source in the microscope is a white LED which works well for bright- and darkfield imaging, but is not ideal for hyperspectral

imaging as certain wavelengths are poorly represented (see Fig. 10). To adjust the focus, coarse and fine focus knobs are present on the microscope. A stepper motor is fixed to the fine focus knob. The stage position may be moved in X and Y directions by manipulating the stage position knobs. By fixing a stepper motor to the X-position knob, stage panning functionality is achieved. This is done using a belt drive from a stepper motor to the knob. For processing samples in the laboratory setup for preliminary testing, two 20 ml syringes are fixed to the microscope with a 3D printed holder, acting as inlets and outlets. The inlet is connected to the pump which in turn is connected to the channel slide. Finally, the outlet of the channel slide is led to the outlet-syringe, where the sample ends up after processing. In an autonomous setting on a USV, the inlet would be connected to a water reservoir.

An Arduino UNO is used as the microcontroller in the system. The microcontroller is flashed with the GRBL v0.9 firmware. A CNC-shield V.3 mates directly to the headers on the Arduino, and has expansion slots for stepper drivers. For this system, DRV8825 stepper drivers are used together with NEMA-17 stepper motors. These stepper motors provide enough torque to manipulate the knobs for focus and stage position.

The pump used in the system is a BOXER 29QQ peristaltic water pump. The pump is available in two motor configurations; a geared DC-motor, or a stepper motor. The latter also comes with the option of an included stepper driver. For this design, the stepper motor version with the included driver is used. The pump can accommodate inner roller tubes of different sizes, and the diameter of the tube affects the flow rate. In this setup, a tube with a diameter of 0.5 mm is used, allowing for flow rates up to 7.8 ml/min. Larger tubes with diameters of 1 mm and 2 mm can also be used, and may be better suited when imaging larger particles. When using the pump with the integrated driver, the pump is connected directly to the headers on the CNC-shield, bypassing the DRV-8825 driver.

For this build, two white label ToupTek-cameras are used. One is a high-speed camera from BRESSER capable of recording at frame rates up to 300 FPS at a resolution of 720x540 pixels. The short exposure time means that the sensor is well suited for capturing images of fast moving particles, as well as imaging under light conditions such as when a darkfield condenser is used. The other camera is from Delta Optical, and is capable of recording at three different resolutions: 640x480, 1280x960, and 2560x1922. Higher resolutions captures more spatial details, but the sampling speed must be reduced as the resolution is increased. For the highest resolutions, the best images are taken when the sample is stationary.

Moreover, a hyperspectral imager (HSI) is connected to the system. The HSI used is a low-cost in-house made push-broom instrument in the visible to near infrared range (400 nm to 800 nm) with approximately 5 nm spectral resolution [10]. As the particles flow by, the HSI collects their spectral signatures, which can further be used for identification and classification of the particles.

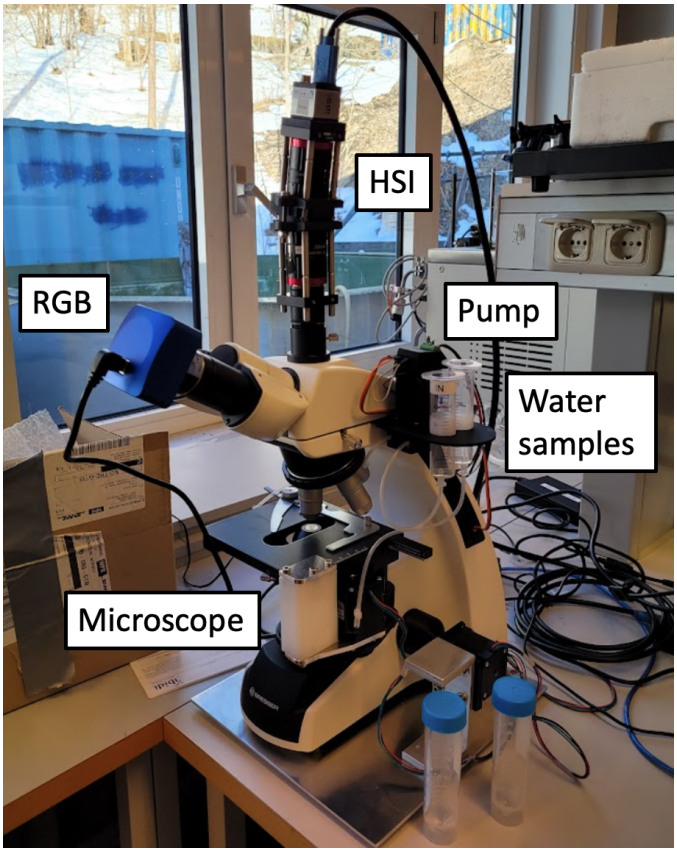

Fig. 2. Assembled AFTI-scope. Sensors are attached to the eyepiece tubes of the microscope. Note that the channel slide is not installed underneath the objective in this picture.

B. Software

The software that controls the system is written in Python, and may be divided between two parts: camera software, and serial software. The camera software is responsible for interfacing with the ToupTek cameras. This includes passing related settings to the camera, as well as receive images from the camera and save them. For debugging purposes, these images can also be displayed to the user in real time. To enable this, the python library PyQt5 is used. PyQt5 is a powerful graphical user interface (GUI) toolkit with features that allow programmers to easily create complex GUIs. Coupled with the software development kit (SDK) from ToupTek, interfacing with the cameras is an easy task.

The serial software is responsible for communicating with the Arduino and CNC-Shield. Based around the python library Pyserial, communication with the Arduino microcontroller is done serially through an USB cable, sending specific GRBL-commands to the Arduino running the firmware. These are translated to stepper signals which in turn actuate the stepper motors and pump in the system.

For testing and debugging, a graphical user interface is designed using PyQT5, shown in figure 3. The GUI allows for camera-, pump- and sample-related settings to be changed. The GUI provides a preview of the camera output, allowing

the focus to be fine tuned prior to sampling. The settings that can be changed include camera exposure time and resolution, pump speed, and sample volume and name. Furthermore, buttons to pump in both directions as well as stop are included. The focus can also be adjusted with dedicated buttons, moving the stage both directions at a resolution of 5 µm. To assist with hyperspectral data capture, several settings such as scan length and scan speed are available. The python program wraps a tool called *ueye-tool* to interface with the hyperspectral sensor. Upon capture, the stage is slowly moved as the sensor scans the slide in a push-broom manner. The cameras used in this design are C-mount microscope cameras. The threaded mounts allow the camera to be fixed directly to the microscope, but these cameras often come with adapters so that they can be installed in the eyepiece tube of the microscope.

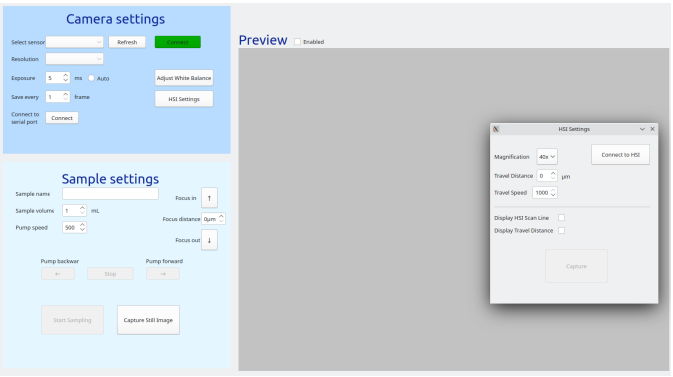

Fig. 3. Graphical User Interface. Camera and sample related settings are changed in the left part of the window. When a camera is connected, a preview can be shown in the gray window. The pop-up menu to the right is for capturing hyperspectral data.

IV. Testing

The system was tested at Trondheim Biological Station during the winter of 2023. Previously, the system was tested with different configurations of pump speeds and channel slide depths, as well as a general benchmarking of the system. This included imaging a micrometer slide to derive the resolution in micrometers/pixel. The testing showed that imaging particles using the deepest slide (0.8 mm) at speeds around 2 ml/min provided an ideal trade-off between flow rate and image quality.

During this test, several samples of phytoplankton collected at earlier occasions were sampled with the AFTI-scope. The samples were originally from waters off Sistranda in the municipality of Frøya, Trøndelag, and were collected from March-June 2022. A plankton net (100 µm mesh size) was deployed from in the upper 5 m of the water column and used to collect and concentrate the water samples. Samples were preserved in neutral lugols at 2% final concentration. Later at the lab, samples were inserted in the AFTI-scope at a pump speed of 1 ml/min, processing approximately 4 ml of each sample. The channel slides had a depth of 800 µm and a magnification of 100x was used. Only the Delta Optical camera recording at 1280x960p was used during this testing.

The hyperspectral imaging was also tested in this setup. In this case, fresh samples from Trondheimsfjord (coast of mid-Norway) were collected at the pier at Trondheim Biological Station using a phytoplankton net (20 µm mesh size). A sub-sample was inserted in the AFTI-scope, which phytoplankton cells flowed through the channel located underneath the objective. Before acquiring hyperspectral images, the flow was stopped, and the hyperspectral camera captured data as it was panned over an object of interest while the RGB camera from Delta Optical captured reference photos.

V. Results

A. Benchmarking

The Delta-optical camera resolution at 40x and 100x magnification are shown in Tables I and II. These results were achieved by imaging a micrometer slide and dividing the observed length by the number of pixels, yielding the resolution in µm/pixel.

TABLE I
Image resolution at 40x magnification

Image size (pixels)	Resolution (µm/pixel)
640x480	4.81
1280x960	2.04
2592x1944	1.02

TABLE II
Image resolution at 100x magnification

Image size (pixels)	Resolution (µm/pixel)
640x480	1.58
1280x960	0.82
2592x1944	0.41

B. RGB Pictures

Selected frames from the Sistranda samples are shown in Fig. 4 through Fig. 9. The different samples depict different cultures of phytoplankton, captured by the Delta Optical RGB-camera as they are pumped through the channel slide. High spatial resolution allows smaller phytoplankton such as *Skeletonema* to be imaged, shown in figure 6.

C. Hyperspectral Data

For the hyperspectral data, the spectral composition of the light source in the microscope was first investigated. The average spectrum in a selection of pixels in the hyperspectral image where no particles were present (box 1 in Fig. 11) in the 400 nm to 800 nm range was plotted and is shown in Fig. 10. It shows that most light is available around 430 nm and between 500 nm to 650 nm, while light close to 400 nm, around 480 nm and above 700 nm is poorly represented. Where there is less light, reflectance and absorbance data will be more noisy, as the signal-to-noise ratio will be considerable lower.

An RGB representation of one of the hyperspectral datacubes can be seen in Fig. 11. Several particles are visible in

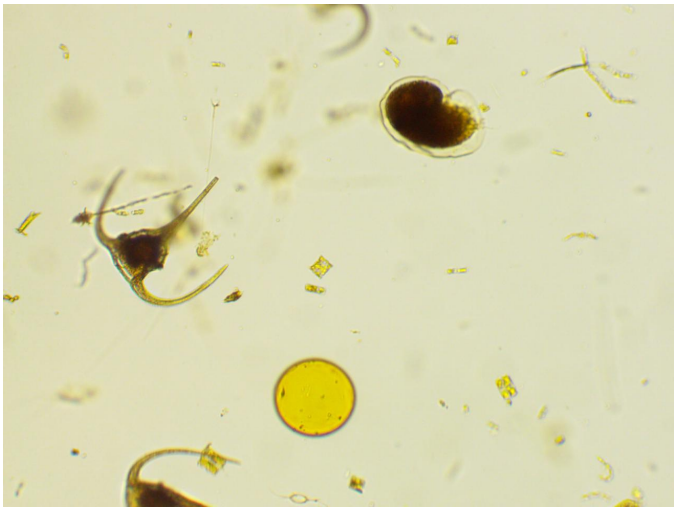

Fig. 4. Image of the dinoflagellate *Tripos* and a zooplankton larva.

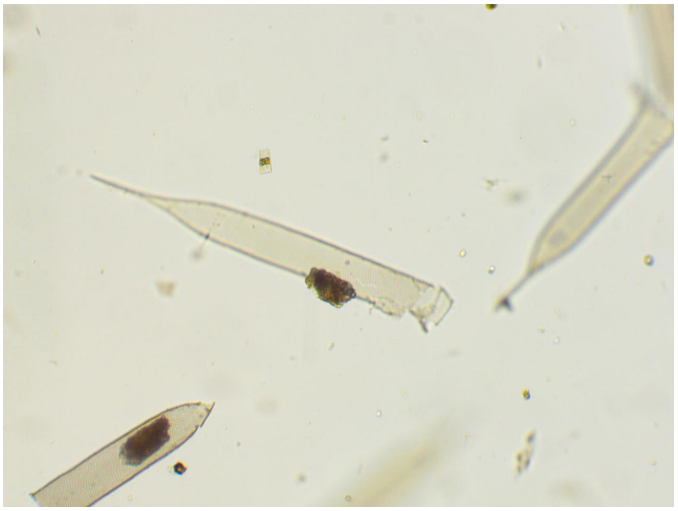

Fig. 5. Image of tintinnid ciliates.

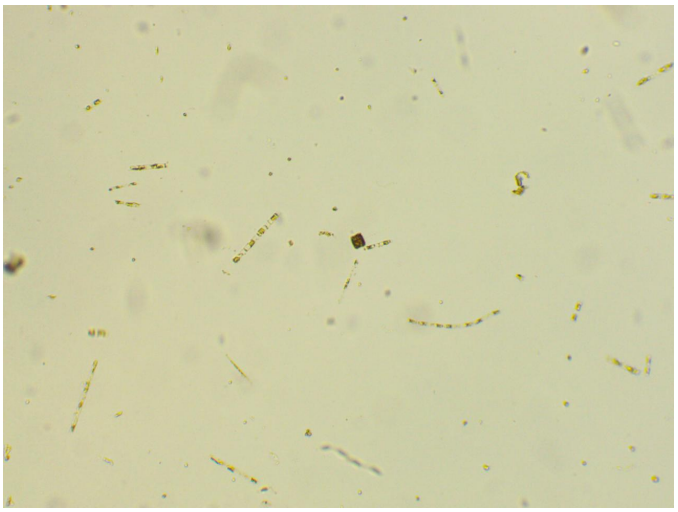

Fig. 6. Image of several specimens of the chain-diatom *Skeletonema*.

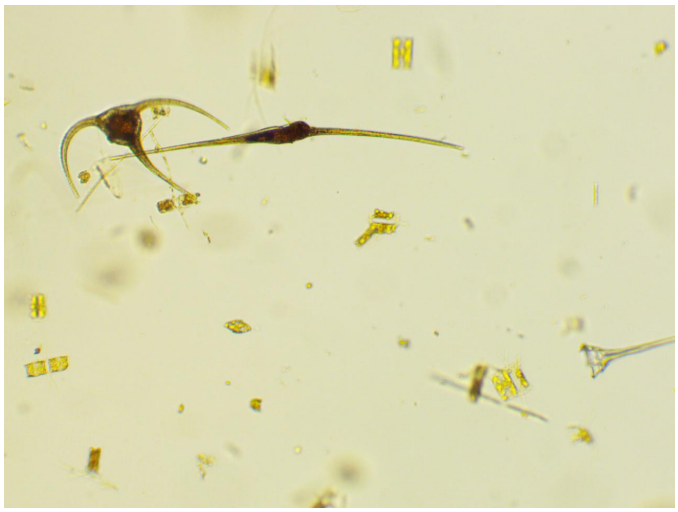

Fig. 7. Image of *Tripos* and diatoms.

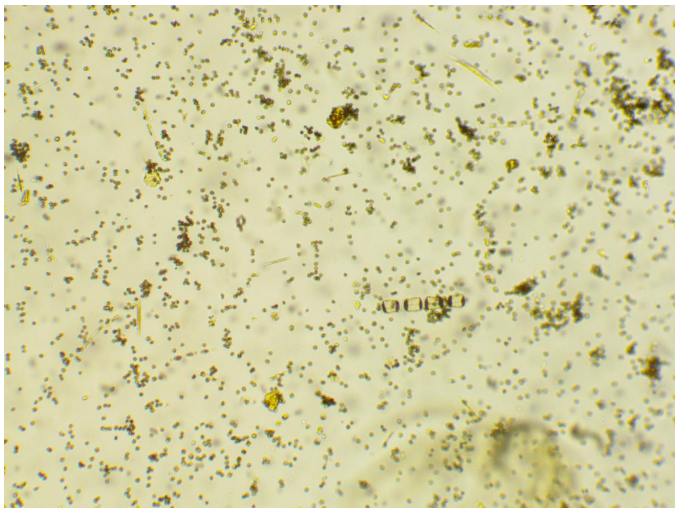

Fig. 8. Image of a concentrated samples where single cells of *Phaeocystis pouchetii* dominates.

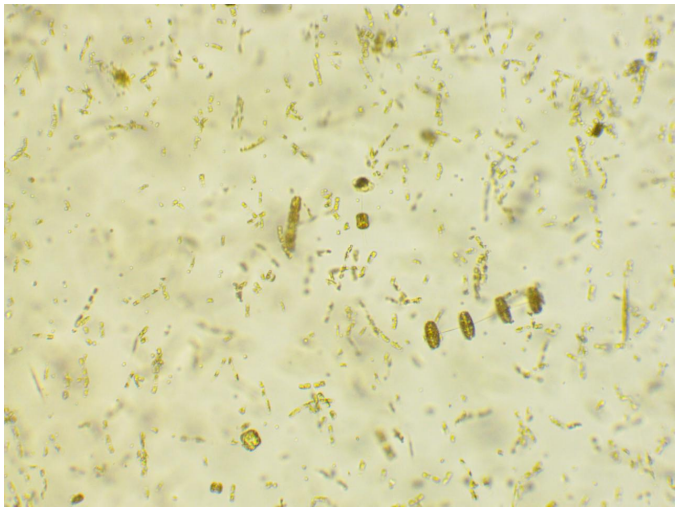

Fig. 9. Images of several chain diatoms, including *Thalassiosira* and *Skeletonema*.

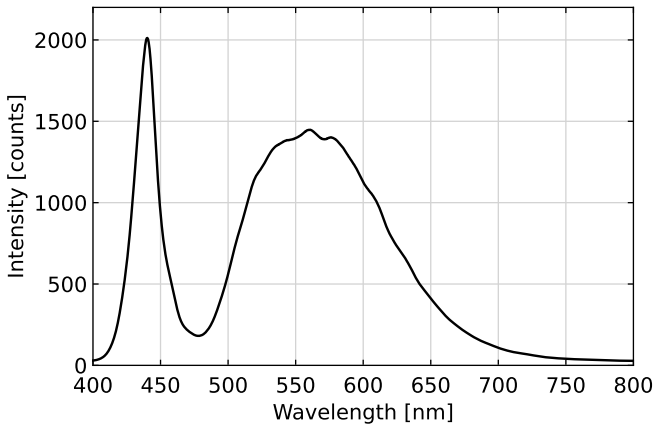

Fig. 10. Spectral composition of the light source in the microscope in the 400 nm to 800 nm range, captured by the HSI.

the image. A selection of the particles (and the background) is further investigated, as marked in red boxes and numbered in the figure. Box 1 shows the background area, particle 2, 3, 4 and 8 are most likely the diatom *Thalassiosira*, particle 5 looks like a fecal pellet, particle 6, 7 and 9 could be the diatom *Chaetoceros*, and particle 10 the diatom *Fragilariopsis*. To further look at the spectra of these particles the background light was removed from the raw data by dividing by the background spectrum, and the spectra normalized by dividing by the maximum pixel value in the image. The resulting spectra are shown in Fig. 12.

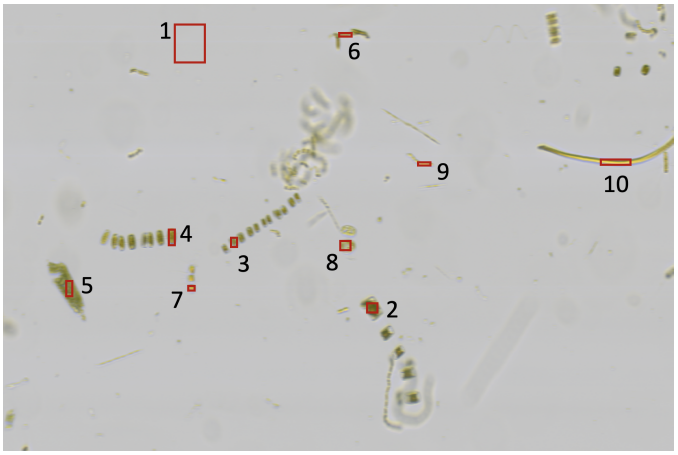

Fig. 11. RGB representation of hyperspectral datacube. Particles selected for further investigation (line plot in figure 12) are marked in red boxes.

The spectra can be compared to known spectra of phytoplankton, or to the typical reflectance or absorbance spectra of different pigments, such as the ones from [12] shown in Fig. 13. For most spectra in Fig. 12 the chlorophyll-a peak at around 675 nm is easily visible, except for in the background (1) and the fecal pellet (5), which makes sense as the chl-a pigment here would degrade. In the diatoms, the shape from carotenoids can be recognized specially in particles 2, 3, 4 and 5, and chlorophyll-c (chl-c) seems also to be present, making

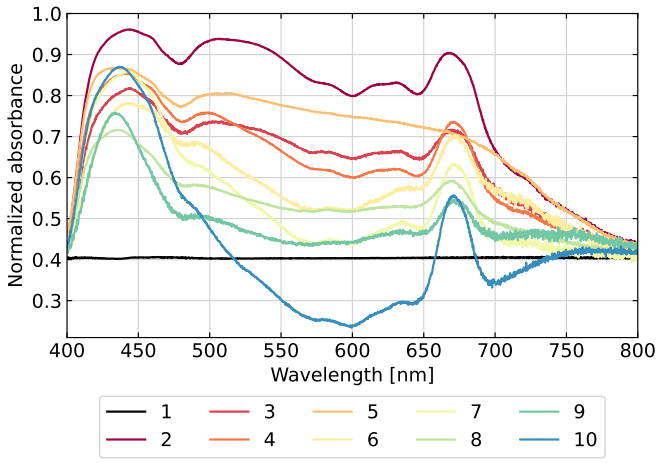

Fig. 12. Spectra of the selected particles in figure 11.

the peak around 450 nm broader, and also peaking at around 580 nm and 640 nm. This is as expected, as diatoms contain the pigments chl-a, chl-c and the carotenoid fucoxanthin [13].

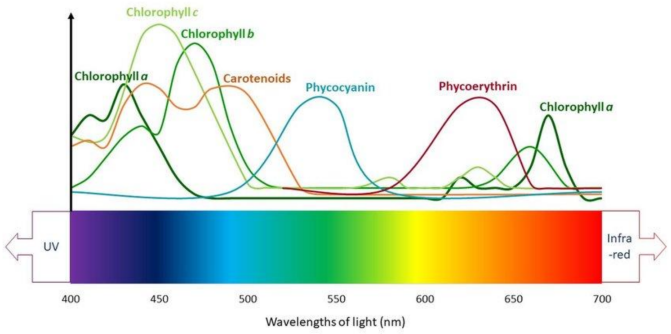

Fig. 13. Absorbance spectra of some pigments typical in phytoplankton [12].

A spectral index such as the normalized difference vegetation index (NDVI) algorithm can also be used to separate pixels containing chlorophyll-a from the pixels without. This is often used in remote sensing applications, such as seen in [14] and [15]. The NDVI is calculated as

$$\frac{NIR - RED}{NIR + RED}, \tag{1}$$

where *RED* is a band in the red part of the spectrum and *NIR* a band in the near infrared. However, since the signal here is very noisy above 700 nm due to little light available, the index was modified to detect the chlorofyll-a peak at 675 nm. The bands *RED*=675 nm and *NIR*=700 nm are therefore used, and the calculation applied to the image in Fig. 11, with the result shown in Fig. 14. A threshold value can be applied to create a mask of these particles. Choosing the threshold value to be 0.25 gives a mask as shown in Fig. 15. This can be used to automatically detect particles in the samples. Furthermore, the spectra of the unmasked pixels can be investigated, and classification be used to sort the particles into different classes

after a model has been trained, or classification could be applied to the whole unmasked images.

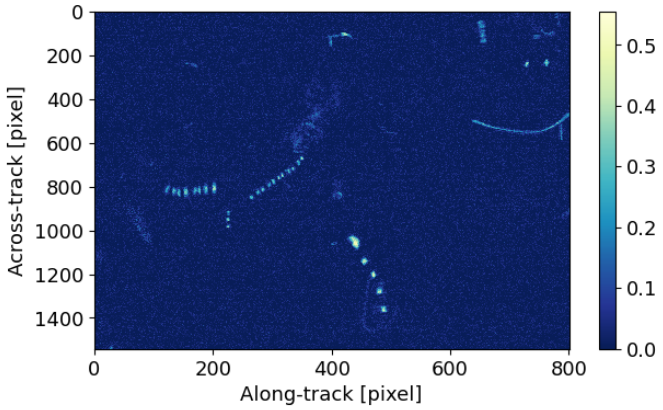

Fig. 14. NDVI calculated using *RED*=675 nm and *NIR*=700 nm.

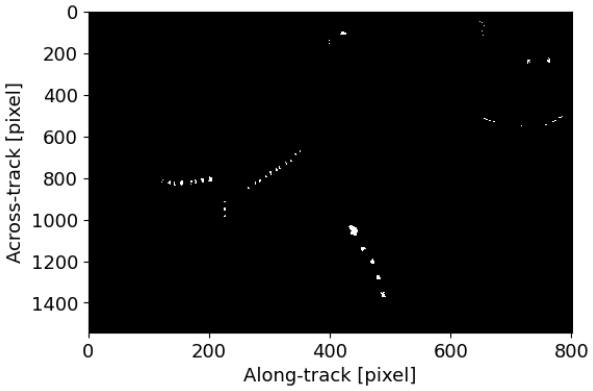

Fig. 15. Mask created from the NDVI plot using a threshold value of 0.25.

VI. Discussion and Conclusion

The AFTI-scope is capable of capturing microscopic images of particles with a resolution of 0.41 µm/pixel at flow rates up to 7.8 ml/min. The eyepiece tubes provide attachment points for any sensor that may interface with a C-mount, demonstrated by attaching a RGB camera and a hyperspectral imager to the system. Water samples were sampled with the AFTI-scope, producing data sets containing images of the particles under magnification. The images could be used to identify the underlying species, and when installed on an autonomous vehicle, such an identification could be carried out remotely. The image data sets can be further processed through post-processing methods such as removing the average image from all the images, efficiently removing any particles stuck to the slide. The background can be normalized, yielding an uniform pixel range. Thresholding can then be used to produce binary masks based on pixel values, similar to the mask created from the NDVI-mask in Fig. 15. Each particle in these masks could be cropped out and subsequently fed into a neural network, possibly allowing classification at lower taxonomic ranks. The integration of a hyperspectral sensor provides additional information through the analysis of spectra related to biological phenomenon. In Fig. 12, peaks around the wavelength of chlorophyll-a are noticeable and consistent with the photosynthesis of the diatoms present in the frame. Certain species have unique spectral signatures that can aid in their identification. The capability of carrying out in-situ identification of suspended particles through the use of autonomous vehicles can enable the classification and quantification of these particles, as well as save resources in terms of personnel and time.

Acknowledgment

This research was supported by the Research Council of Norway through the Center of Excellence AMOS (grant number 223254), MoniTARE project (grant number 315514), the IKTPLUSS project AWAS (grant number 327670), and the interdisciplinary project HYPSCI (grant number 325961).

Thanks to Dennis Langer for the utility to automate data capture with the hyperspectral sensor through the Ueye-tool.

References

[1] Rodger, H.D., Henry, L. and Mitchell, S.O. “Non-infectious gill disorders of marine salmonid fish“. *Rev Fish Biol Fisheries*, 21, 423–440 , 2011. https://doi.org/10.1007/s11160-010-9182-6

[2] Grant Stephen D., Richford Kyle, Burdett Heidi L., McKee David and Patton Brian R., “Low-cost, open-access quantitative phase imaging of algal cells using the transport of intensity equation“, 2020. R. Soc. open sci.7:191921 191921 http://doi.org/10.1098/rsos.191921

[3] Pollina T, Larson AG, Lombard F, Li H, Le Guen D, Colin S, de Vargas C, Prakash M “PlanktoScope: Affordable Modular Quantitative Imaging Platform for Citizen Oceanography“, *Frontiers in Marine Science* 9. 2022. doi: 10.3389/fmars.2022.949428

[4] Simon Martin Schroeder. the MorphoCut image processing library. url: https://morphocut.readthedocs.io/en/stable/index.html (visited on 9th April 2023)

[5] EcoTaxa. url: https://ecotaxa.obs-vlfr.fr (visited on 9th April 2023)

[6] Saad, A., E. Davies, and A. Stahl, “Recent Advances in Visual Sensing and Machine Learning Techniques for in-situ Plankton-taxa Classification“. *Ocean Sciences Meeting*, 2020.

[7] Sosik, H.M. and R.J. Olson, “Automated taxonomic classification of phytoplankton sampled with imaging-in-flow cytometry.“ *Limnology and Oceanography: Methods*, 2007. 5(6): p. 204-216.

[8] Harred, L.B. and L. Campbell, “Predicting harmful algal blooms: a case study with Dinophysis ovum in the Gulf of Mexico.“ *J. Plankton Research*, 2014. 36(6): p. 1434-1445.

[9] Fabien Lombard et al, “Globally Consistent Quantitative Observations of Planktonic Ecosystems.“ *Frontiers in Marine Science* 6. 2019, doi: 10.3389/fmars.2019. 00196.

[10] M. B. Henriksen, E. F. Prentice, C. M. van Hazendonk, F. Sigernes, T. A. Johansen, “Do-it-yourself VIS/NIR pushbroom hyperspectral imager with C-mount optics“, *Opt. Continuum*, vol. 1, pp. 427-441, 2022

[11] F. Sigernes, M. Surjäsuo, R. Storvold, J. Fortuna, M. E. Grøtte, T. A. Johansen, “Do it yourself hyperspectral imager for handheld to airborne operations“, *Optics Express*, Vol. 26, pp. 6021-6035, 2018; https://doi.org/10.1364/OE.26.006021

[12] Roy, S., Llewellyn, C. A., Egeland, E. S., and Johnsen, G. (Eds.). “Phytoplankton pigments: characterization, chemotaxonomy and applications in oceanography“. *Cambridge University Press*, 2011.

[13] J. Berge, G. Johnsen, and J. H. Cohen. “Polar Night Marine Ecology“. Springer, 2020.

[14] Kim, E.-J.; Nam, S.-H.; Koo, J.-W.; Hwang, T.-M. “Hybrid Approach of Unmanned Aerial Vehicle and Unmanned Surface Vehicle for Assessment of Chlorophyll-a Imagery Using Spectral Indices in Stream“, South Korea. Water 2021, 13, 1930. https://doi.org/10.3390/w13141930

[15] Song, B.; Park, K. “Detection of Aquatic Plants Using Multispectral UAV Imagery and Vegetation Index“, *Remote Sensing*, Vol. 12, pp. 387, 2020 https://doi.org/10.3390/rs12030387